

Scattering mechanisms and electronic transport properties in a $\text{Hg}_{1-x}\text{Cd}_x\text{Te}$ medium-infrared detector

A. El-Abidi^{*1}, A. Nafidi¹, H. Chaib¹, A. Taoufik

¹Laboratory of Condensed Matter Physics and Nanomaterials for Renewable Energy, Department of Physics, Faculty of Sciences, BP 8106 Hay Dakhla; University Ibn Zohr, 80000 Agadir, MOROCCO.

(*) Corresponding author. E-mail: elabidiabderrahim@yahoo.fr; nafidi21@yahoo.fr

Abstract: We report here transport properties measurements and theoretical results on modeling carrier charge mobility in $\text{Hg}_{1-x}\text{Cd}_x\text{Te}$ ($x=0.22$). Conductivity and Hall Effect were measured in the temperature range 4.2 - 300 K. Our measurements indicate that the sample is n-type semiconductor. In intrinsic regime, the slope of the curve $R_H T^{3/2}$ indicates a gap of 178 meV which agree well with E_g ($x = 0.22$, 300 K) = 183 meV. Our theoretical calculations, according to the Kane model, show that the Fermi energy E_F increases with temperature. The calculated donor state E_d is 3 meV above the conduction band at 4.2 K and agrees well with 0.67 meV of low field Hall effect measurements. Our theoretical calculations on the mobility shows that ionized impurity scattering dominate below 25 K, optical phonons scattering at high temperatures (>70K) and the mobility is generated by the both mechanisms of scattering in the intermediate temperature regime. At high temperatures, an excellent agreement between experimental and calculated scattering mobility is obtained by introducing a trial function. The detection wave length $\lambda = 6.89 \mu\text{m}$ situates the sample as medium-infrared detector.

PACS:

Keywords: $\text{Hg}_{1-x}\text{Cd}_x\text{Te}$, Hall Effect, conductivity, scattering, transport mobility.

I. Introduction

The level of development achieved in the growth technics of semiconductor has allowed the experimental observation of a number of fine aspects present in optical and transport properties of these structures. Among them The II-VI ternary random alloys $\text{Hg}_{1-x}\text{Cd}_x\text{Te}$ have been predicted as a stable alternative for application in infrared optoelectronic devices. Especially in the region of second atmospheric window (around 10 μm) which is of great interest for communication. A number of papers have been published devoted to the band structure of this system as well as its magneto optical properties [1]. A study on the temperature dependence respectively of Hall constant, conductivity, and mobility reveals the importance of scattering mechanisms. The aim of this work is to determine the transport properties for $\text{Hg}_{1-x}\text{Cd}_x\text{Te}$ ($x=0.22$) and the contribution of various scattering mechanisms by doing theoretical curve fitting on the experimental temperature-mobility plot.

II. Experimental methods

The $\text{Hg}_{1-x}\text{Cd}_x\text{Te}$ sample was grown by molecular beam epitaxy (MBE) on [111] CdTe substrate. The nominal composition ($x = 0.22$) was determined by density measurements with a precision of ± 0.005 in x . The Hall Effect measurements and conductivity were done in the

temperature range 4.2-300K. A weak current ($I = 0.1 \text{ mA}$) flows along the sample under a transversal weak magnetic field ($B = 0.2 \text{ T}$). The Ohmic contacts were obtained by chemical deposition of gold from a tetrachloroauric acid in methanol solution after a proper masking to form the Hall crossbar.

III. Theory and general formulation

The calculation of the Fermi energy E_F at a temperature T have been done via the formula (1) giving the expression of the density n of electrons in the conduction band. We iterated on the value of E_F between 0 and $E_g + 10 k_B T$, that gives a density n near of the measured one n_{mes} .

$$n = \frac{2}{\sqrt{\pi}} N_c \int_0^\infty \frac{(E)^{1/2}}{1 + e^{(E-E_F)/k_B T}} dE \quad (1) \quad \text{where: } \eta = \frac{E_F - E_c}{k_B T} \text{ and } N_c = 2 \left(\frac{2\pi m^* k_B T}{h^2} \right)^{3/2}. \quad k_B \text{ is the Boltzmann's constant.}$$

The energy gap has been calculated by the empiric formula of G. Hansen et al [2]:

$$E_g(x, T) = -0.302 + 1.93x - 0.810x^2 + 0.832x^3 + 5.03510^{-4}(1-2x)T \quad (2)$$

Here T is the temperature in Kelvin, E_g is the material band gap in eV and x is the fractional composition value. The effective mass of electron m^* was obtained via Kane model band [3].

$$m^* = \frac{1}{-0.6 + 6.333 \left(\frac{2}{E_g} + \frac{1}{E_g + 1} \right)} m_0 \quad (3) \quad m_0 \text{ is the free-electron mass}$$

The effective mass of hole was fixed at $m_h = 0.55 m_0$ [4]. The origin of energies is taken at the top of the valence band ($E_v = 0$ and $E_c = E_g$). The carrier concentration n_{mes} was calculated from the standard expression:

$$n_{mes} = \frac{r_H}{|R_H| \cdot e} \quad (4) \quad \text{For convenience } r_H \text{ was assumed to be unity.}$$

In order to determine the energy of the donor level E_d , we iterated in the formula (5) - giving the expression of E_F as a function of the temperature [5] - on values of E_d that vary between 0 and $E_g + 5 k_B T$. The E_d energy is therefore the one that gives the E_F calculated previously. The calculation of E_d have been done in extrinsic regime ($4.2K \leq T \leq 77K$).

$$\left\{ \begin{array}{l} * \text{ For : } k_B T < E_g/10 \\ E_F = E_d + k_B T \ln \left\{ \frac{1}{4} \left[-1 + \left(1 + 8 \frac{N_d}{N_c} e^{(E_c - E_d)/k_B T} \right)^{1/2} \right] \right\} \\ * \text{ For : } k_B T > E_g/10 \\ E_F = \frac{E_c + E_v}{2} + \frac{k_B T}{2} \ln \frac{N_v}{N_c} \end{array} \right. \quad (5)$$

The density of donor impurities in the sample was $N_c = n_{mes} = 5.24 \cdot 10^{14} \text{ cm}^{-3}$ in the regime of carriers freeze-out.

Electron mobility has been calculated in the temperature rang $4.2K \leq T \leq 300K$ by the solution of the Boltzmann equation with the relaxation-time approximation [6]

$$\vec{\nabla} \cdot \vec{grad}_r f + \frac{1}{\hbar} \vec{F} \cdot \vec{grad}_k f = - \frac{f - f_0}{\tau(\vec{k})} \quad (6)$$

We included four types of scattering processes namely, acoustic phonons scattering, piezoelectric scattering, polar optical phonons scattering and ionized impurity scattering. The Hall mobility $\mu_H = |R_H \cdot \sigma_0|$, where R_H is the Hall coefficient and σ_0 the conductivity without field, will be compared to the calculated electron mobility μ .

The relations between electron mobility and temperature, for various scattering processes, are given as follows:

The acoustic phonons scattering mobility is given by the relation [7]:

$$\mu_{ac} = \frac{3 \cdot 10^{-5} C_1}{\left(\frac{m^*}{m_0} \right)^{5/2} T^{3/2} E_{ac}^2} \quad (7)$$

Where: $C_1 = 6.97 \cdot 10^{10} \text{ N.m}^{-2}$ [8] is the longitudinal elastic constant, $E_{ac} = 9.5 \text{ eV}$ [8] is the deformation potential for acoustic phonons.

The piezoelectric scattering mobility is given by the relation [9]:

$$\mu_{pz} = 2.6 \frac{\epsilon_s}{(m/m_0)^{3/2} k^2 (T/100)^{1/2}} \quad (8) \quad \epsilon_s \text{ is the}$$

dielectric static constant in the semiconductor and is given by the relation [4]: $\epsilon_s = 20.5 - 15.5 x + 5.7 x^2$ (9),

ϵ_0 is the dielectric constant in vacuum and k' is given

$$\text{by: } k' = \frac{e_{pz}}{\sqrt{e_{pz}^2 + \epsilon_0 \cdot \epsilon_s \cdot C_1}} \quad (10) \quad \text{where } e_{pz} \text{ is the}$$

piezoelectric constant. The polar optical phonons scattering mobility is given by the relation [9]:

$$\mu_{op} = 2.6 \cdot 10^5 \frac{\exp\left(\frac{\theta_D}{T}\right)}{\alpha \cdot (m^*/m_0) \cdot \left(\frac{\theta_D}{k'}\right)} \quad (11)$$

Where θ_D is the Debye's temperature and α is the coupling constant without dimension given by:

$$\alpha = \frac{1}{137} \sqrt{\frac{mc^2}{2k_B \theta}} \left(\frac{1}{\epsilon_{op}} - \frac{1}{\epsilon_s} \right) \quad (12)$$

ϵ_{op} is dielectric optical constant. α is 0.39 for CdTe and 0.05 for HgTe [10]. The Debye's temperatures of HgTe and CdTe are respectively 147.5 K [11] and 160 K [12]. When the alloy $\text{Hg}_{1-x}\text{Cd}_x\text{Te}$ is a two mode system in which the optical modes associated with CdTe and with HgTe are both observed, the mobility was calculated from Eq. (11) by first substituting the CdTe values for the appropriate parameters, then using the values for HgTe in the expression and averaging the two results [10] with the expression: $\frac{1}{\mu_{op}} = \frac{x}{\mu(\text{CdTe})} + \frac{1-x}{\mu(\text{HgTe})}$ (13) The

ionized impurity scattering mobility μ_{imp} is given by the Brooks-Herring equation [13]:

$$\mu_{imp} = \frac{3.28 \cdot 10^{15} \epsilon_s^2 T^{3/2}}{(N_a + N_d) (m^*/m_0)^{1/2} \left[\ln(b+1) - \frac{b}{b+1} \right]} \quad (14)$$

Where: $b = \frac{1.29 \cdot 10^{14} (m^*/m_0) \epsilon_s T^2}{N^*}$ (15) and N^* is the effective screening density given by:

$$N^* = n + \frac{(n + N_a)(N_d - N_a - n)}{N_d} \quad (16) \quad \text{Where } N_a \text{ and } N_d \text{ are,}$$

respectively, the concentration of acceptors and donors. The total mobility μ is calculated using the relation:

$$\frac{1}{\mu} = \sum_i \frac{1}{\mu_i} \quad (17) \quad \text{where } \mu_i \text{ refers to the individual}$$

calculated mobility from various scattering processes and i is the number of scattering process included.

IV. Results and discussion

The measurement of R_H at different temperatures shows that the sample is an n-type semiconductor in fig.1.

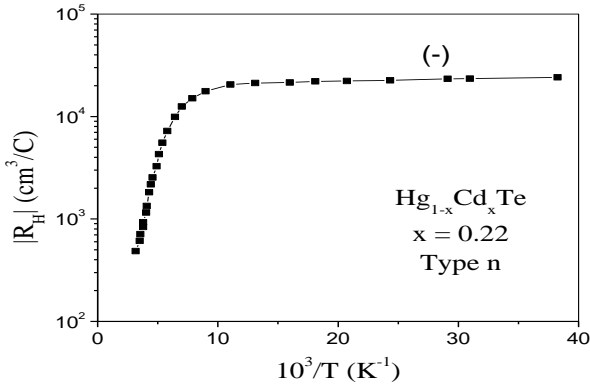


Fig. 1: Temperature dependence of the Hall constant in $\text{Hg}_{1-x}\text{Cd}_x\text{Te}$ ($x=0.22$).

At low temperature (in extrinsic regime), we are in presence of a carrier freeze-out and the density of the carriers is nearly independent of the temperature. After R_H increases slightly according to $10^3/T$ following the diminution of the density of carriers as described by:

$$n \propto \exp\left(-\frac{\Delta E_d}{2k_B T}\right) \quad [9], \quad \Delta E_d = E_c - E_d \text{ is the}$$

full activation energy. The slope of $|R_H| = f(10^3/T)$ curve in extrinsic regime in fig.1 allow us to determinate the donor ionisation energy $\Delta E_d = -0.67$ meV. That shows the existence of a donor state at 0.67 meV above the conduction band.

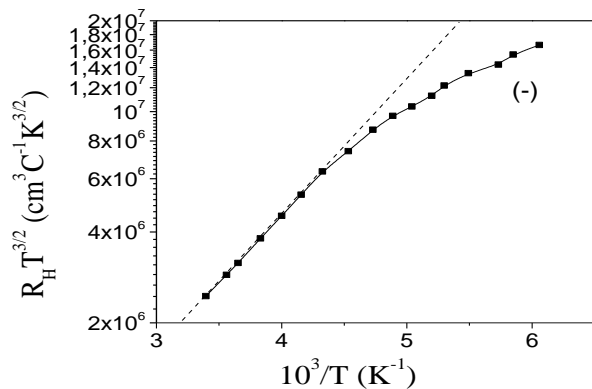


Fig.2: variation of $R_H \cdot T^{3/2}$ as a function of $10^3/T$ in $\text{Hg}_{1-x}\text{Cd}_x\text{Te}$ ($x=0.22$).

When the temperature increases, in the intrinsic regime, the electrons go thermally from the donor level (caused by Te rather than Hg interstitials [14]) and valence band to the conduction band. So the carrier's concentration increases and Hall constant decreases. The slope of $|R_H T^{3/2}|$ ($10^3/T$) in fig.2 gives $E_g = 178$ meV which agree well with $E_g(300\text{K}, x=0.22) = 184$ meV, given by the formula of Hansen et al. The corresponding detection wave length to this small gap is $\lambda = 6.89 \mu\text{m}$. This

situates the sample as medium-infrared detector (MIR) as shown in the fig. 3.

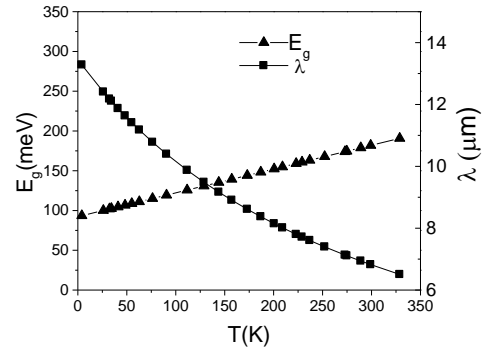


Fig. 3 Temperature dependence of the band gap E_g and cut-off wavelength λ

The measured electrons concentration n_{mes} at 4.2 K, 77 K and at the ambient temperature 300 K, and their corresponding calculated Fermi energy are given in Tab.1 and shown in the fig 4.

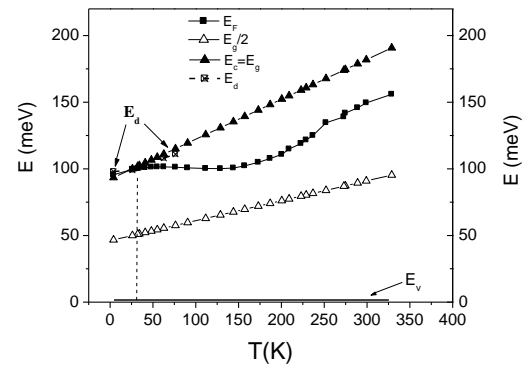


Fig.4 Fermi energies versus temperature

$T(\text{K})$	$n_{\text{mes}} (\text{cm}^{-3})$	$E_F (\text{meV})$
4	$(2.5 \pm 0.3) \cdot 10^{14}$	97
77	$(3.01 \pm 0.36) \cdot 10^{14}$	103
280	$(1.03 \pm 0.12) \cdot 10^{16}$	151

Tab.1 : The concentration of electrons and the energy of Fermi at different temperatures.

$T(\text{K})$	$E_g (\text{meV})$	$E_d (\text{meV})$
4.2	95.2	98
77	116.9	111

Tab.2: Calculated E_g and E_d at 4.2K and 77K.

At low temperatures (25 K-100 K), the thermal energy is sufficient to ionize all donors and one reaches a plateau of concentration of carriers. This allows us to extract the

density N_D : $n = N_D - N_A = N_D = 5.24 \cdot 10^{14} \text{ cm}^{-3}$.

And to determine the donors energy level's E_d in Tab.2.

In our calculations we found an electronic donor state approximately at 3 meV above the conduction band at $T = 4.2$ K. A resonant electronic state 8 meV above the conduction band at 4.2 K was observed in Shubnikov de Hass experiments in $\text{Hg}_{0.8}\text{Cd}_{0.2}\text{Te}$ [15] which is different to 0.67 meV from our Hall experiments and the calculated 3 meV.

For the intrinsic conduction $\sigma_0 = |e| n_i \mu_h (1+b)$ where $b = \mu_e / \mu_h$. Since the intrinsic concentration n_i rises exponentially with temperature to $n_i = \sqrt{N_C N_V} \cdot \exp(-E_g / 2 K_B T)$; we obtain the temperature dependence of σ_0 as shown in Fig.5. When the temperature is lowered, σ_0 enters the extrinsic region where the carrier concentration is constant and σ_0 rises, for the simplest case $\sigma_0 \propto \tau_0 \propto T^{-3/2}$. At still lower temperatures, there is a carrier freeze-out.

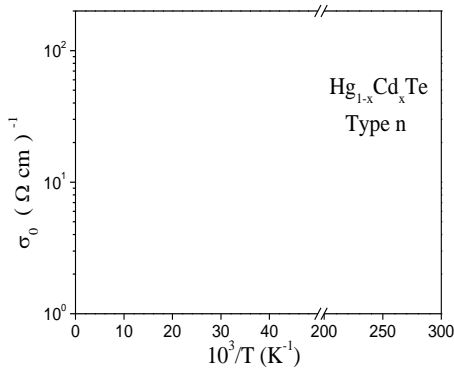


Fig.5: Temperature dependence of the conductivity in the investigated $\text{Hg}_{1-x}\text{Cd}_x\text{Te}$ ($x = 0.22$)

In Fig. 6 we see the effect of single-scattering mechanisms on the total electron mobility. Ionized impurity scattering is seen to dominate below 25 K, optical phonons scattering at high temperatures ($>70\text{K}$) and the mobility is generated by the both mechanisms of scattering in the intermediate temperature regime.

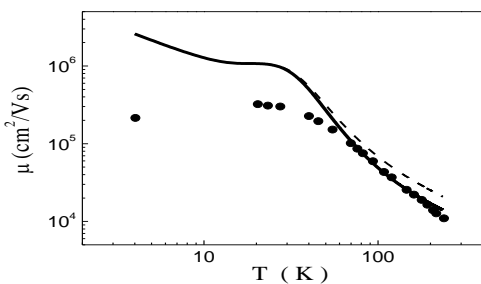


Fig.6: Temperature dependence of the mobility. The closed circles represent the experimental data points. The dashed curve represent the sum of all contributions of

various scattering mechanisms while the solid line represents the sum taken into account the additional term.

At lower temperatures the calculated mobility is about a factor of 10 greater than the measured value. This disagreement can be due to the impurities type acceptors and the non-parabolicity of the conduction band not taken into account in our calculations. The discrepancy is reduced at higher temperatures to a factor of 1.3.

In order to improve the agreement between theory and experiment, in the intrinsic regime, we added a term which replaces additional scattering mechanisms not discussed in this paper such as electron-hole scattering and scattering by optical transversal phonons. We tried to estimate such a term by a trial function: $\mu_a = \mu_1 \exp(\mu_2/T)$ [16] where $\mu_1 = 15835 \text{ cm}^2 \text{ V}^{-1} \text{ s}^{-1}$ and $\mu_2 = 239 \text{ K}$ are fitting parameters. These values have been determined while minimizing the sum of squares which characterizes the quality of the fit. In fig. 7, the additional term within these values gives a good agreement for temperatures higher than 70 K.

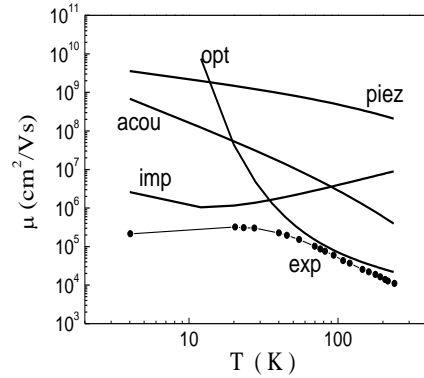


Fig.7: Electron mobility as a function of temperature. The closed circles represent the experimental data. The various other curves refer to calculated contributions of various scattering mechanisms.

V. Conclusions

We have presented transport properties measurements and theoretical results on Fermi energy, donor state energy and mobility of $\text{Hg}_{1-x}\text{Cd}_x\text{Te}$ ($x = 0.22$). Calculated electron mobilities are observed to be in agreement with experimental data points at high temperatures. On the contrary, a discrepancy is observed at the low temperatures what is due to the non compatibility of the singly ionized donor scattering centres model and the non parabolicity of the conduction band which is not taken into account. However, we can conclude that the ionized impurity scattering dominate below 25 K, optical phonons scattering at high temperatures ($>70\text{K}$) and the mobility is generated by the both mechanisms of scattering in the intermediate temperature regime. The average of Hall mobility is $2.7 \cdot 10^5 \text{ cm}^2/\text{Vs}$ at low temperature. This agrees well with the fact that for small x the alloy had electronics

properties near these of bulk HgTe. This sample is a medium-infrared detector. We are trying to fit such mobility in p-type $\text{Hg}_{1-x}\text{Cd}_x\text{Te}$ ($x=0.204$) [17] and in the two-dimensional (II-VI) p-type HgTe/CdTe superlattice [18].

References

- [1] J. L. Schmit, J. Appl. Phys. 41 (1990) 2876.
- [2] L. Hansen, J.L. Shmit, T.M. Casstleman, J. Appl. Phys. Vol 53, p7099-7101 (1982).
- [3] M.A. Kinch, M.J Brau, A. Simmons, J. Appl. Phys.44 (1973)1649
- [4] Wenus J. Rutkowski J., Rogalski A., IEEE trans. On electron devices, vol. 48, 7, p1326-1332 (2001).
- [5] P. Kiéev, Semiconductor physics, (Mir, Moscou, 1975), Chap. 3, P. 213
- [6] A. El-Abidi., doctorate thesis, Ibn zohr university, Agadir Morocco (2010)
- [7] F. J. Blatt, in Solid state physics, edited by F. Seitz and D. Turnbull (Academic, New York, 1957), vol.4, p. 332.
- [8] D. Chattopadhyay and B.R. Nag, Journal of applied physics, Vol. 45, NO. 3, March 1974
- [9] K. Seeger, Semiconductor physics, an introduction (Springer, 2002), chap 6 p.159-221.
- [10] W. Scott J. Appl. Phys., Vol. 43, No. 3, March 1972
- [11] J G Collins et al 1980 J. Phys. C: Solid State Phys. **13** 1649-1656
- [12] T F Smith et al 1975 J. Phys. C: Solid State Phys. **8** 2031-2042
- [13] J. D. Wiley, Semiconductors and semimetals (Vol. 10), Academic Press, New York (1975).
- [14] R. Dornhaus, H. Happ, K.H. Müller, G. Nimtz, W. Schlabit, P. Zaplinski, G. Bauer: in proc. XIIthInt. Conf. Phys. Semicond., Stuttgart 1974, ed . by M.H. Pilkuhn (Teubner, Stuttgart 1974), p.1157.
- [15] R. Dornhaus, G. Nimtz, W. Schlabit, H. burkhard : Solid State Commun. 17, 837 (1975).
- [16] P.Moravec, R Grill, J Franc, R Vaghova, P Höschl and E Belas..semicond.Sci. Tecghnol. 16 (2001) 7-13
- [17] A. El Abidi, A. Nafidi et al, Book of Abstracts (CA:235) 10th Moroccan Meeting On the chemistry of The state Solide (REMCES 10) Meknes, Morocco, April 27, 28 and 29 (2005)
- [18] A. El Abidi, A. Nafidi et al, Physica B: Physics of Condensed Matter 405, (2010) pp 936-940